10.24425/acs.2026.1543

Archives of Control Sciences
Volume 36(LXXII), 2026
No. 2*, pages 425–446*

Adaptive synergetic MPPT controller for optimal performance of photovoltaic systems

Khalissa BEHIH, Nadjat ZERROUG, Ziyad BOUCHAMA, Najib ESSOUNBOULI, Abdelhak BENHENICHE and Fouad ZEBIRI

This paper presents a novel optimization strategy for photovoltaic (PV) power systems based on a synergetic control (SC) theory integrated with state observation and adaptive estimation schemes. The main objective is to enhance system reliability and reduce implementation costs through the elimination of selected physical sensors. A state observer is designed to ensure stable system operation and avoid control-law singularities, while adaptive laws are employed to accurately estimate the load and the photovoltaic output voltage. These estimated states are provided to the synergetic controller, which drives the system to operate at the maximum power point (MPP). The proposed strategy is validated through numerical simulations under dynamic conditions, including variations in solar irradiance, temperature, and load. Furthermore, experimental tests corroborate the simulation results, confirming the robustness and high efficiency under partial shading conditions and demonstrating the strategy's practicality for real-world PV systems.

Key words: adaptive observer, maximum power point tracking, photovoltaic systems, partial shading, renewable energy, synergetic control

K. Behih (corresponding author, e-mail: khalissabehih@univ-setif.dz) is with the Department of Electrical Engineering and LSI Laboratory, University of Sétif 1, Ferhat Abbas, Algeria.

N. Zerroug (e-mail: nadjatzerroug@univ-setif.dz) is with the Department of Electrical Engineering and QUERE Laboratory, University of Sétif 1, Ferhat Abbas, Algeria.

Z. Bouchama (corresponding author, e-mail: ziyad.bouchama@univ-bba.dz) is with the Department of Electromechanical Engineering, University of Bordj Bou Arreridj, and QUERE Laboratory, Algeria.

N. Essounbouli (e-mail: najib.essounbouli@univ-reims.fr) is with the CReSTIC Laboratory, University of Reims Champagne-Ardenne, France.

A. Benheniche (e-mail: abdelhak.benheniche@univ-bba.dz) is with the Department of Electromechanical Engineering, University of Bordj Bou Arreridj, and QUERE Laboratory, Algeria.

F. Zebiri (e-mail: f.zebiri@univ-bba.dz) is with the Department of Electromechanical Engineering and LPMRN Laboratory, University of Bordj Bou Arreridj, Algeria.

Received 10 January 2026. Revised 14 April 2026. Accepted 19 May 2026.

1. Introduction

Recently, the use of renewable energy has emerged as a promising and sustainable solution to reduce the global energy crisis and restrain the adverse effects of environmental degradation [1–4]. Solar energy is one of the most popular types of renewable energy and stands out due to its cleanliness, abundance, and widespread availability, offering a viable and eco-friendly alternative to conventional fossil fuel-based power generation [5, 6]. Despite these advantages, the performance of photovoltaic (PV) systems often remains constrained, since their low energy conversion efficiency depends on several factors such as solar irradiation, temperature variations, load fluctuations, and the physical characteristics of the PV modules. Overcoming these limitations is crucial to enhancing the viability of solar energy.

To enhance the energy yield of PV systems under varying operating conditions, numerous control strategies have been developed, among which Maximum Power Point Tracking (MPPT) algorithms play a principal role. These algorithms ensure optimal power extraction by continuously adjusting the operating point of the PV system. However, traditional MPPT techniques, such as Perturb and Observe (P&O) and Incremental Conductance (IC) [7–11], suffer from several drawbacks, including persistent oscillations around the maximum power point, difficulty in distinguishing the true maximum power point under partial shading conditions, and reliance on multiple sensors, which increases system complexity [12].

Given the highly nonlinear nature of PV system dynamics, advanced nonlinear control strategies and intelligent control methods have been explored to overcome these limitations. Among nonlinear techniques, Sliding Mode Control (SMC) is well-known for its robustness and disturbance rejection capabilities [13–16]. Nevertheless, conventional SMC is deteriorated by chattering, high-frequency oscillations that can damage system components and degrade overall performance. As a powerful alternative, Synergetic Control (SC) has emerged, offering similar robustness with a simpler design and the inherent ability to generate smooth, chatter-free control signals [17–19]. Despite these advantages, a common drawback of both SMC- and SC-based approaches is their reliance on multiple sensors, which raises system cost and implementation complexity. Similarly, while intelligent methods such as fuzzy logic and neural networks can effectively handle nonlinearities [18, 20], their high computational demand and need for extensive training make them impractical for many cost-sensitive or real-time embedded applications.

This paper proposes and evaluates an innovative control strategy that enhances both the performance and practicality of MPPT for PV systems. The main contribution lies in the development of an Adaptive Synergetic Control (ASC) technique, integrated with a state observer to estimate and compensate for system uncertainties and external disturbances. The proposed ASC-MPPT is an observer-based synergetic control strategy rather than a gradient-based MPPT method [19, 21–23], since it regulates the operating point through a Lyapunov-designed macro-variable and adaptive state estimation. This approach addresses the following key issues. First, unlike strategies that employ cascaded controllers (one to compute the PV reference voltage and another to enforce it), this work introduces a simplified control design that significantly lowers algorithmic complexity. Second, it tackles the problem of observing the DC-DC converter output voltage without relying on directly measured initial values, which in many existing works leads to singularities in the control law unless the output capacitor is pre-charged (an assumption that is not always practical in real conditions). Third, the proposed ASC-MPPT controller minimizes the number of sensors by eliminating the need for a direct PV output voltage measurement, thereby reducing system cost and hardware requirements. Finally, while many experimental studies neglect practical shading scenarios [19, 21–24], this work explicitly considers partial shading tests, thereby validating the robustness of the proposed controller under realistic and challenging operating conditions.

2. Dynamic Photovoltaic System Description

The nonlinear photovoltaic system, shown in Fig. 1, consists of a PV array connected to a load via a DC-DC boost converter. The dynamic model of the PV system is derived under necessary assumptions to make it suitable for nonlinear controller design. When the boost converter operates in conduction mode, the

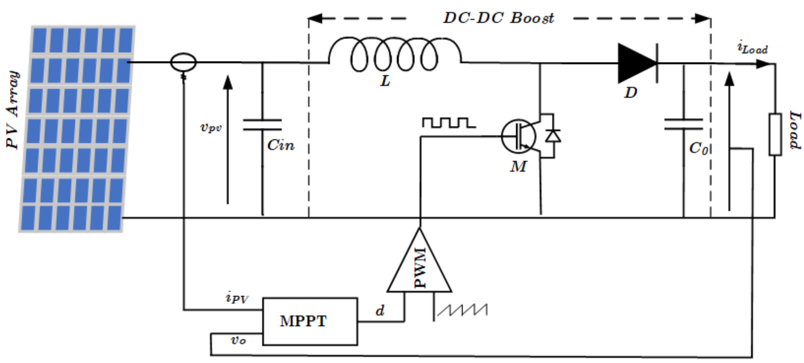

Figure 1: Schematic diagram of a photovoltaic system with an MPPT controller

system can be described as follows:

$$\begin{aligned}\dot{i}_{pv} &= -\frac{(1-d)}{L}v_0 + \frac{v_{pv}}{L}\,,\\ \dot{v}_0 &= \frac{(1-d)}{C_o}i_{pv} - \frac{v_0}{RC_o}\,,\end{aligned} \tag{1}$$

where i_{pv} is the photovoltaic current, v_0 is the boost output voltage and d is the necessary control signal to be designed. The positive constants L, R, C_{in} and C_0 represent the inductance, load resistance, input capacitance, and output capacitance, respectively.

Selecting the photovoltaic current and the output voltage as system state variables, i.e, $y = \begin{bmatrix} i_{pv} & v_0 \end{bmatrix}^{\mathrm{T}}$, and letting $\zeta_1 = i_{\mathrm{load}} = v_0 R^{-1}$ denote the load current and $\zeta_2 = v_{pv}$ denote the photovoltaic voltage, the state-space averaged model can be rewritten as:

$$\begin{aligned}\dot{y}_1 &= -\frac{(1-d)}{L}y_2 + \frac{\zeta_2}{L}\,,\\ \dot{y}_2 &= \frac{(1-d)}{C_o}y_1 - \frac{\zeta_1}{C_o}\,.\end{aligned} \tag{2}$$

As given in equation (2), the dynamic model of the PV system is independent of its load nature, remaining valid across many load types while still capturing the correct operating point imposed by the load demand. This yields a unified and compact model that is easier to analyze and control.

3. Adaptive Synergetic MPPT Controller Design

The main objective is to develop an MPPT controller to generate a pulse width modulation (PWM) signal by adjusting its duty cycle to extract maximum power, compensating for fluctuations caused by environmental changes or load disturbances. In this design approach, the control strategy integrates a state observer with adaptive estimation schemes. The observer reconstructs the photovoltaic current and output voltage while simultaneously providing real-time estimates of the photovoltaic voltage and load current. In this context, the dynamic model (2) is rewritten as given in (3):

$$\begin{aligned}\dot{\hat{y}}_1 &= -\frac{(1-d)}{L}\hat{y}_2 + \frac{\hat{\zeta}_2}{L} + \kappa_1\left(y_1 - \hat{y}_1\right)\,,\\ \dot{\hat{y}}_2 &= \frac{(1-d)}{C_o}\hat{y}_1 - \frac{\hat{\zeta}_1}{C_o} + \kappa_2\left(y_2 - \hat{y}_2\right)\,,\end{aligned} \tag{3}$$

where $\kappa_1 > 0$ and $\kappa_2 > 0$ are the observer gains, and $\hat{y}_1$ and $\hat{y}_2$ are the observer's average states. The variables $\hat{\zeta}_1$ and $\hat{\zeta}_2$ represent the estimates of the unknown load current and photovoltaic voltage, respectively. Subtracting (3) from (2) yields the dynamics of the estimation errors:

$$
\begin{aligned}
\dot{\widetilde{y}}_1 &= -\frac{(1-d)}{L}\widetilde{y}_2 + \frac{\widetilde{\zeta}_2}{L} - \kappa_1 \widetilde{y}_1 \,, \\
\dot{\widetilde{y}}_2 &= \frac{(1-d)}{C_o}\widetilde{y}_1 - \frac{\widetilde{\zeta}_1}{C_o} - \kappa_2 \widetilde{y}_2 \,.
\end{aligned}
\tag{4}
$$

To derive the adaptation laws for $z\hat{e}ta_1$ and $z\hat{e}ta_2$, consider the Lyapunov function candidate in (5).

$$
V = \frac{1}{2}L\widetilde{y}_1^2 + \frac{1}{2}C_o\widetilde{y}_2^2 + \frac{1}{2r_1}\widetilde{\zeta}_1^2 + \frac{1}{2r_2}\widetilde{\zeta}_2^2 \,, \tag{5}
$$

where $r_1 > 0$ and $r_2 > 0$ are design parameters. Then, the time derivative of (5) can be expressed as:

$$
\dot{V} = L\widetilde{y}_1\dot{\widetilde{y}}_1 + C_o\widetilde{y}_2\dot{\widetilde{y}}_2 - \frac{1}{r_1}\widetilde{\zeta}_1\dot{\hat{\zeta}}_1 - \frac{1}{r_2}\widetilde{\zeta}_2\dot{\hat{\zeta}}_2 \,, \tag{6}
$$

Substitution of equation (2) and (3) into (5) yields:

$$
\dot{V} = -\kappa_1 L\widetilde{y}_1^2 - \kappa_2 C_{\mathrm{out}}\widetilde{y}_2^2 - \widetilde{\zeta}_1\left[\widetilde{y}_2 + \frac{1}{r_1}\dot{\hat{\zeta}}_1\right] + \widetilde{\zeta}_2\left[\widetilde{y}_1 - \frac{1}{r_2}\dot{\hat{\zeta}}_2\right], \tag{7}
$$

The adaptation laws are selected as follows:

$$
\begin{aligned}
\dot{\hat{\zeta}}_1 &= -r_1\widetilde{y}_2 \,, \\
\dot{\hat{\zeta}}_2 &= r_2\widetilde{y}_1 \,,
\end{aligned}
\tag{8}
$$

which leads to:

$$
\begin{aligned}
\dot{V} &= -\kappa_1 L\widetilde{y}_1^2 - \kappa_2 C_o\widetilde{y}_2^2 \\
&\leqslant 0.
\end{aligned}
\tag{9}
$$

By applying LaSalle's invariance principle [25] to the derived Lyapunov function, the equilibrium point of the observer dynamics is proven to be asymptotically stable. For the PV system, the control law objective is to drive the circuit with a desired photovoltaic current $i_{pv}^* = y_1^* = \hat{y}_2\hat{\zeta}_1\hat{\zeta}_2^{-1}$. To achieve this propriety, the synergetic control synthesis begins by defining the dynamics of the macro-variable, as described in equation (10).

$$
\hat{\sigma} = \hat{y}_1 - y_1^* \,. \tag{10}
$$

To ensure asymptotic stability and convergence to $\hat{\sigma} = 0$, the desired dynamic evolution of the macro-variable can be designed as:

$$\dot{\hat{\sigma}} + \tau\hat{\sigma} = 0, \tag{11}$$

where $\tau > 0$ is design parameter. Then, differentiating the macro-variable in (10) along (3) and combining it with equation (11) leads to (12):

$$-\frac{(1-d)}{L}\hat{y}_2 + \frac{\hat{\zeta}_2}{L} + \kappa_1\widetilde{y}_1 = -\tau\hat{\sigma}\,. \tag{12}$$

Solving for the control law d, leads to (13):

$$d = 1 - \hat{y}_2^{-1}\left(\hat{\zeta}_2 + \kappa_1 L\widetilde{y}_1 + \tau L\hat{\sigma}\right). \tag{13}$$

To guarantee the synergetic design, the initial conditions for the observer $(\hat{y}_1(0), \hat{y}_2(0))$ and the adaptation laws $\left(\hat{\zeta}_1(0), \hat{\zeta}_2(0)\right)$ must be chosen appropriately. Specifically, the macro-variable must be zero initially, a condition satisfied by setting $\hat{\sigma}(0) = \hat{y}_1(0) - \hat{y}_2(0)\hat{\zeta}_1(0)\hat{\zeta}_2^{-1}(0)$.

4. Stability analysis

Assumptions

The photovoltaic I–V characteristic is continuous and locally Lipschitz in the operating region of interest, while irradiance and temperature are bounded and vary at bounded rates. The converter parameters L, C_o, and R are positive and belong to known bounded intervals representing practical tolerances. The measured current is bounded and filtered so that switching noise does not destabilize the observer. The design parameters κ_1, κ_2, r_1, r_2, and τ are strictly positive. Consequently, the closed-loop plant-observer system is well defined and admits solutions for all $t \geqslant 0$.

Proposition 1. *Consider the MPPT problem of the PV system (1). In synergetic mode, the closed-loop system consisting of (2), (4), (7) and (13) is asymptotically stable, with the estimated variable converging to its equilibrium values* (ζ_1, ζ_2).

Proof. Without loss of generality, rewriting the second equation of the dynamic observer system (3) as:

$$\frac{d\hat{y}_2^2}{dt} = 2\hat{y}_2\frac{(1-d)}{C_o}\hat{y}_1 - 2\frac{\hat{\zeta}_1}{C_o}\hat{y}_2 + 2\kappa_2\left(y_2 - \hat{y}_2\right)\hat{y}_2\,. \tag{14}$$

Now, consider the control law (13) in synergetic mode (i.e., $\hat{\sigma} = 0$). This yields:

$$(1-d) = \hat{\zeta}_2\hat{y}_2^{-1}. \tag{15}$$

Substituting (15) into (14) and using (7), then simplifying and introducing the PV power and load power terms, yields:

$$\frac{d\hat{P}^2_{\text{load}}}{dt} = \frac{2\hat{\zeta}_1^2}{C_o}\left(P_{mmp} - \hat{P}_{\text{load}}\right) + \phi, \tag{16}$$

where ϕ, P_{mmp} and $\hat{P}_{\text{load}}$ denote the auxiliary observer error term, the maximum power point, and the estimated load power, respectively, and are defined as follows:

$$\begin{aligned} \hat{P}_{\text{load}} &= \hat{\zeta}_1\hat{y}_2\,, \\ P_{mmp} &= \zeta_2 y_1^*, \\ \phi &= 2\hat{\zeta}_1\hat{y}_2\left(\kappa\hat{\zeta}_1 - r_1\hat{y}_2\right)\widetilde{y}_2\,. \end{aligned} \tag{17}$$

Since $\widetilde{y}_1 \to 0$ and $\widetilde{y}_2 \to 0$, it follows that $\phi \to 0$. Therefore, the solution to (15) is asymptotically stable, and the controller drives the load power exponentially toward the PV power, ensuring $\hat{P}_{\text{load}} \to P_{mmp}$. As a result, from (4) and (17), the estimates satisfy $\hat{\zeta}_1 \to \zeta_1$ and $\hat{\zeta}_2 \to \zeta_2$.

Remark 1. *Equation (16) describes the dynamics of the estimated load power $\hat{P}_{\text{load}} = \hat{\zeta}_1\hat{y}_2$. Neglecting the perturbation term ϕ and linearizing near the equilibrium $\hat{P}_{\text{load}} \approx P_{mmp}$ yields the error dynamics:*

$$\begin{aligned} \varepsilon &= \left(P_{mmp} - \hat{P}_{\text{load}}\right), \\ \frac{d\varepsilon}{dt} &= \frac{\hat{\zeta}_2^2}{C_o P_{mmp}}\varepsilon. \end{aligned} \tag{18}$$

At the maximum power point, $\hat{\zeta}_2 \to v_{pv}$ and $P_{mmp} = i_{pv}v_{pv}$. Using the power balance and the boost converter voltage relationship $v_0 = v_{pv}(1-d)^{-1}$, Eq. (19) is obtained:

$$\frac{v_{pv}}{i_{pv}} = R(1-d)^2. \tag{19}$$

Consequently, the estimated load power converges to the true maximum power with an approximate exponential rate:

$$\frac{d\varepsilon}{dt} = \frac{R(1-d)^2}{C_o}\varepsilon. \tag{20}$$

Thus, the closed-loop time constant is $C_o\left[R(1-d)^2\right]^{-1}$. To ensure that the observer dynamics are faster than the controlled system, the observer gains should be selected as:

$$\kappa_i \succ\succ \frac{1}{R_{\min}(1-d_{\max})^2 C_o}\,, \tag{21}$$

where $R_{\min}$ is the minimum expected load resistance and $d_{\max}$ is the corresponding duty cycle.

5. Results and discussion

This section provides a comprehensive analysis of the numerical simulation and experimental results for the proposed MPPT controller, highlighting its dynamic and steady-state performance under various operating conditions. In the numerical simulations, the designed robust adaptive MPPT controller is compared with existing synergetic controller designs [19, 21–23]. For both the numerical simulation and experimental setups, the photovoltaic generation used in this study was the Kyocera KC200GT solar panel, which is commonly adopted in MPPT performance evaluations [26, 27]. The boost converter was designed with the following parameters: $L = 0.74$ μH, $C_o = 220$ μF and $C_{\text{int}} = 440$ μF. The load resistance was a minimum of $R = 18$ Ω, and the switching frequency was set to 25 kHz. The ASC-MPPT controller parameters were chosen as $\kappa_1 = \kappa_2 = 2000$ and $\tau = 0.6$.

5.1. Numerical simulation results

The numerical simulation studies incorporate variations in solar irradiance G (Wm^{-2}), temperature T (°C), and load disturbances (Ω), the effects of which are evident in the P–V characteristics shown in Fig. 2.

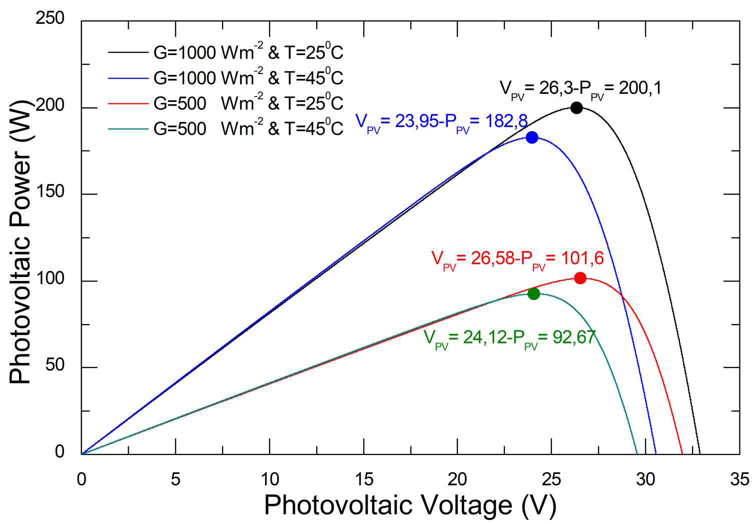

Figure 2: P–V characteristics under various weather operating conditions

The results obtained with the proposed ASC-MPPT controller are compared with those of the SC-MPPT design, in which the macro-variable manifold is defined as follows:

$$\sigma = \frac{\partial P_{pv}}{\partial i_{pv}} = \frac{\partial \left(v_{pv} i_{pv}\right)}{\partial i_{pv}} = i_{pv} \frac{\partial v_{pv}}{\partial i_{pv}} + v_{pv} = 0. \tag{22}$$

Subsequently, the synergetic control strategy determines the control law SC-MPPT, as defined in equation (23).

$$d_{sc} = 1 - \frac{v_{pv}}{v_0} - \frac{L\left(v_{pv} + i_{pv}\dfrac{\partial P_{pv}}{\partial i_{pv}}\right)}{\tau v_0 \left(2\dfrac{\partial P_{pv}}{\partial i_{pv}} + i_{pv}\dfrac{\partial^2 v_{pv}}{\partial^2 i_{pv}}\right)}. \tag{23}$$

Equation (23) indicates that the implementation of the conventional synergetic MPPT controller requires three dedicated sensors, thereby introducing additional system complexity and measurement uncertainty. Moreover, the denominator contains two critical quantities, the output voltage v_0 and the partial derivative (24)

$$\left(2\frac{\partial P_{pv}}{\partial i_{pv}} + i_{pv}\frac{\partial^2 v_{pv}}{\partial^2 i_{pv}}\right). \tag{24}$$

Both of which must remain non-zero to ensure the control law's validity. This critical constraint leads to excessively large control efforts, particularly under low initial output voltage conditions or when the partial derivative term approaches zero.

5.1.1. Simulation Case 1

The system response to an irradiance step change between 1000 Wm^{-2} and 500 Wm^{-2} at a constant temperature of 25°C is shown in Fig. 3 to 6.

The ASC-MPPT controller maintains power levels closer to the MPP and responds more rapidly to irradiance step changes, resulting in higher steady-state power (Fig. 3). Furthermore, its smoother duty cycle signal (Fig. 4) minimizes voltage and current ripples and reduces transient overshoot (Figs. 5 and 6), confirming its enhanced tracking efficiency and robustness.

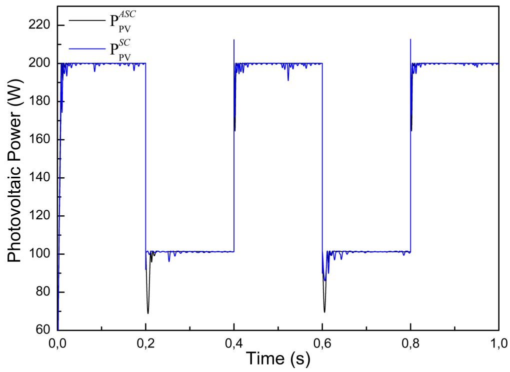

Figure 3: Photovoltaic power evolution in simulation case 1

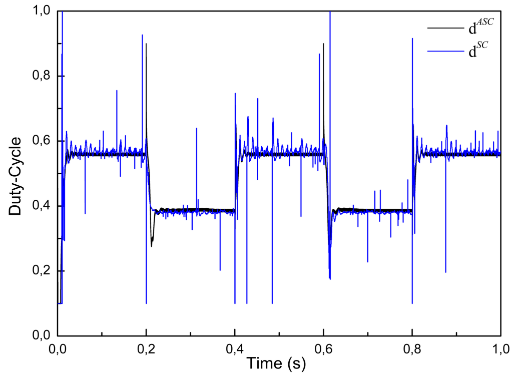

Figure 4: Duty-cycle evolution in simulation case 1

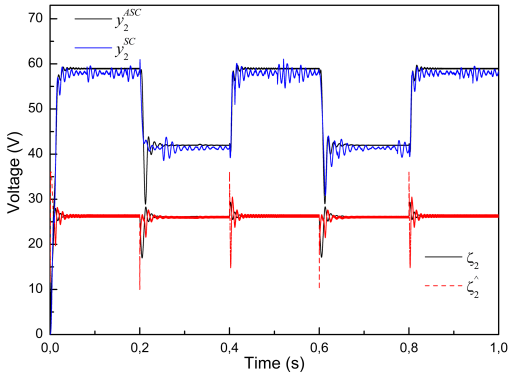

Figure 5: System voltages evolution in simulation case 1

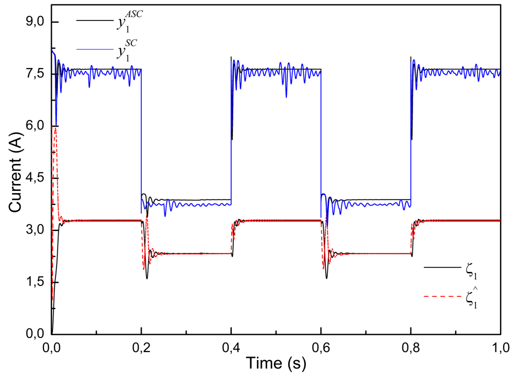

Figure 6: System currents evolution in simulation case 1

5.1.2. Simulation Case 2

At an elevated temperature of 45°C under the previous irradiance profile, the performance of the proposed ASC-MPPT controller is evaluated in the subsequent figures.

In the case of the elevated temperature under the same previous irradiance variation, the ASC-MPPT controller consistently outperforms the SC-MPPT controller, extracting more stable maximum power at the new MPP with minimal ripple, as seen in Fig. 7. The duty cycle profile in Fig. 8 again reveals a smoother control action and reduced transient excursion compared to the SC-MPPT, which improves system efficiency. Furthermore, the proposed controller maintains robust tracking of the voltage and current, keeping their evolutions (Figs. 9, 10)

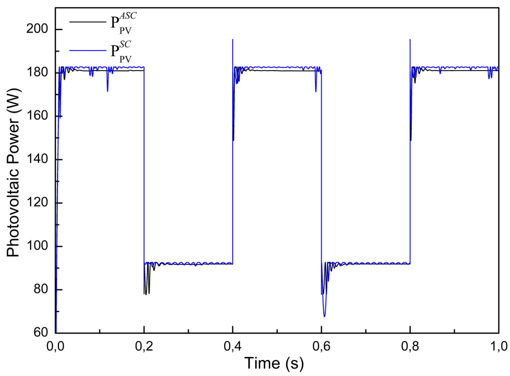

Figure 7: Photovoltaic power evolution in simulation case 2

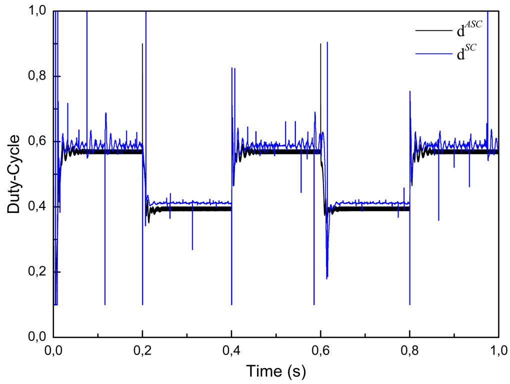

Figure 8: Duty-cycle evolution in simulation case 2

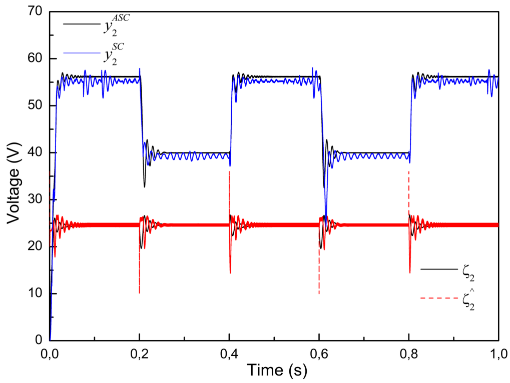

Figure 9: System voltages evolution in simulation case 2

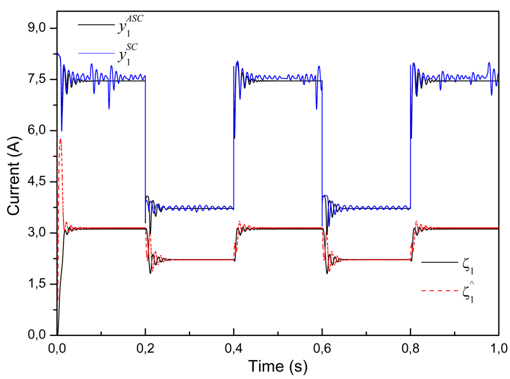

Figure 10: System currents evolution in simulation case 2

near to the reference values. This confirms its robust adaptation to temperature effects and a stable approach to the shifted MPP operating point.

5.1.3. Simulation Case 3

This case demonstrates the controller's robustness under load steps, with constant irradiance 1000 Wm^{-2} and temperature 25°C. The efficiency of the proposed ASC-MPPT controller is compared against the conventional SC-MPPT method.

In this scenario, the ASC-MPPT scheme adjusts the duty cycle with lower control effort during transients compared to the SC method. This maintains PV system operation at the MPP, resulting in smaller transient power loss and demonstrating improved disturbance rejection, as depicted in Figs. 11 and 12. Furthermore, the system voltages and currents (Figs. 13, 14) remain more stable under ASC, confirming closed-loop robustness to load steps, which is critical for grid-interactive or storage-coupled operation.

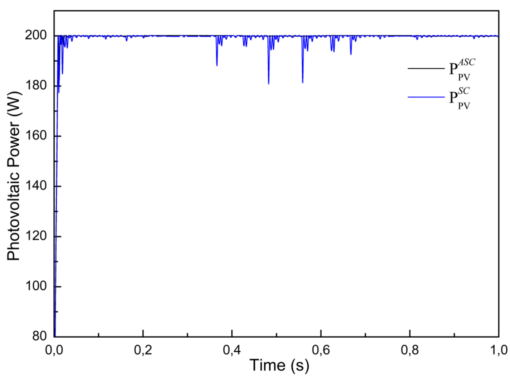

Figure 11: Photovoltaic power evolution in simulation case 3

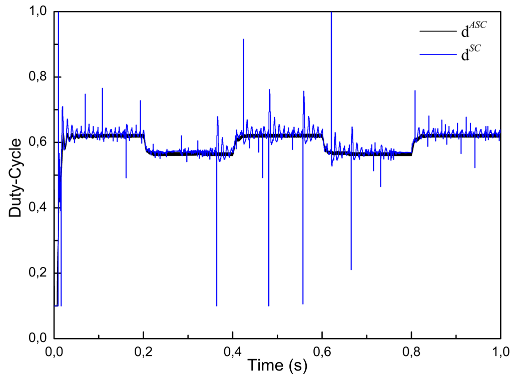

Figure 12: Duty-cycle evolution in simulation case 3

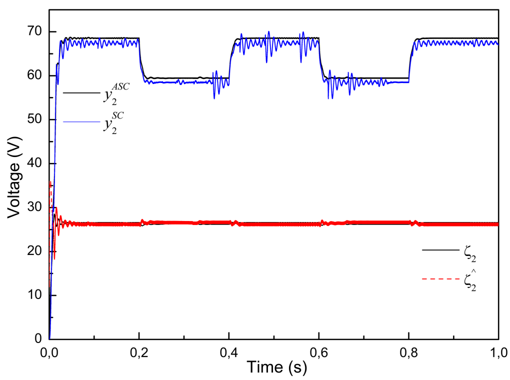

Figure 13: System voltages evolution in simulation case 3

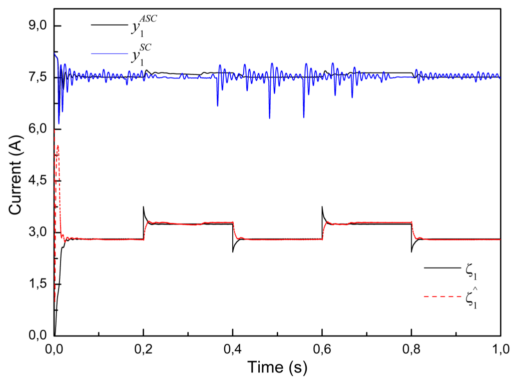

Figure 14: System currents evolution in simulation case 3

As indicated in Table 1, compared with SC-MPPT, the proposed ASC-MPPT provides more stable PV power tracking in all three simulation cases. It consistently reduces ripple and overshoot, improves tracking efficiency, and achieves faster settling times.

Table 1: Performance comparison of ASC-MPPT and SC-MPPT under the three simulation scenarios

Scenario	Method	Efficiency (%)	Settling time (s)	Ripple (%)	Overshoot (%)
Case 1	ASC-MPPT	99.50	0.015	0.20	0.50
	SC-MPPT	98.80	0.028	0.80	1.20
Case 2	ASC-MPPT	99.20	0.018	0.30	0.70
	SC-MPPT	98.10	0.035	1.00	1.50
Case 3	ASC-MPPT	99.70	0.012	0.10	0.30
	SC-MPPT	98.5	0.022	0.60	1.00

5.2. Experimental result

The experimental controller was implemented on a dSPACE DS1104 real-time platform. Since the observer relies on the measured current signal, a soft first-order low-pass filter was applied to attenuate high-frequency switching noise and avoid state jitter. The filter was implemented with a sampling time of 50 µs and a time constant of 5 µs, corresponding to a cutoff frequency of 200 kHz. An experimental PV system has been built using the same circuit and ASC controller parameters as in the previous simulation step. A range of operating scenarios was considered in this section, including unknown weather conditions, load variations, and partial shading. For those operating points, experimental P–V characteristics are obtained as shown in Fig. 15.

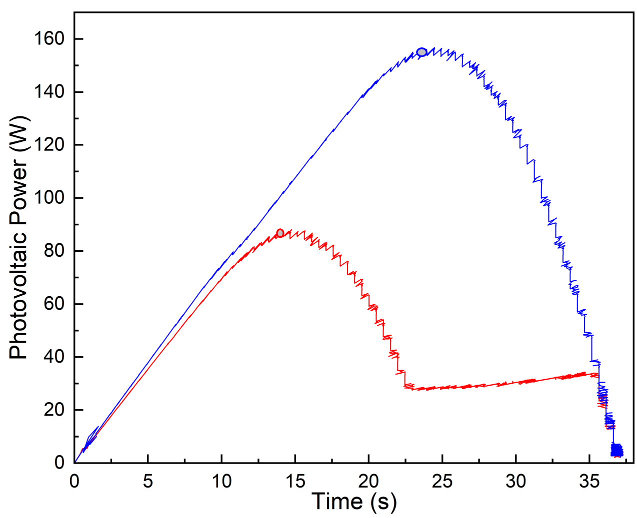

Figure 15: Experimental P–V characteristics

5.2.1. Experimental Case 1

In this case an unknown stable weather condition is considered, the P–V characteristic (blue curve) of which is shown in Fig. 15.

As shown in Fig. 16, the proposed controller maintains the PV power at around 154 W, successfully tracking the maximum power point with a smooth duty cycle, as illustrated in Fig. 17. Furthermore, Figs. 18 and 19 demonstrate that the ASC accurately estimates the PV voltage and load current without direct measurement.

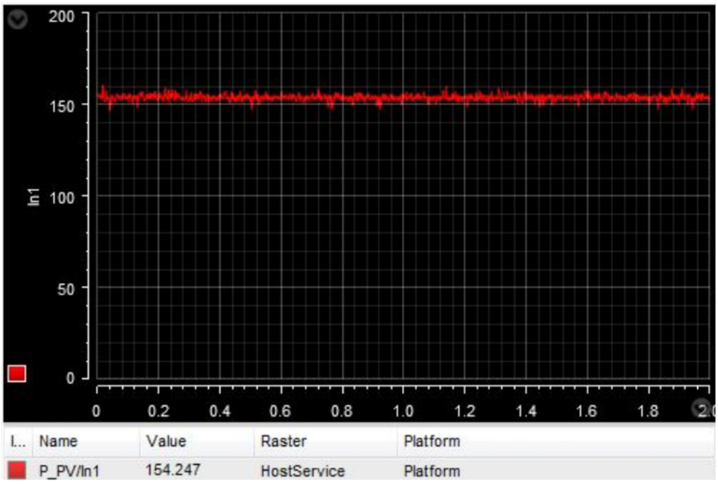

Figure 16: Photovoltaic power evolution in experimental case 1

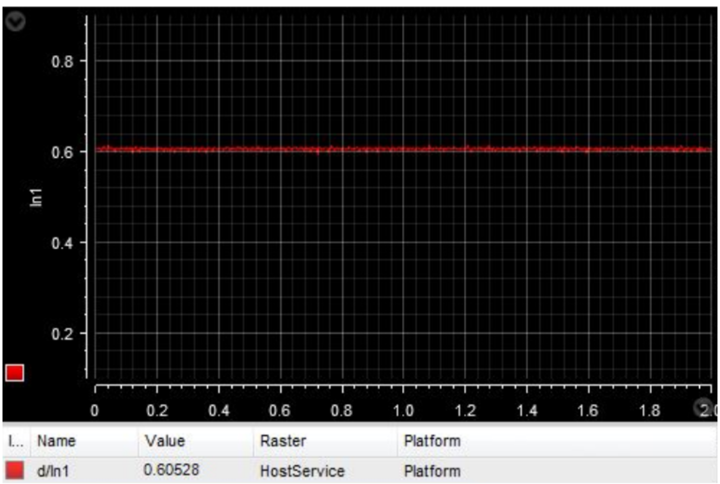

Figure 17: Duty-cycle evolution in experimental case 1

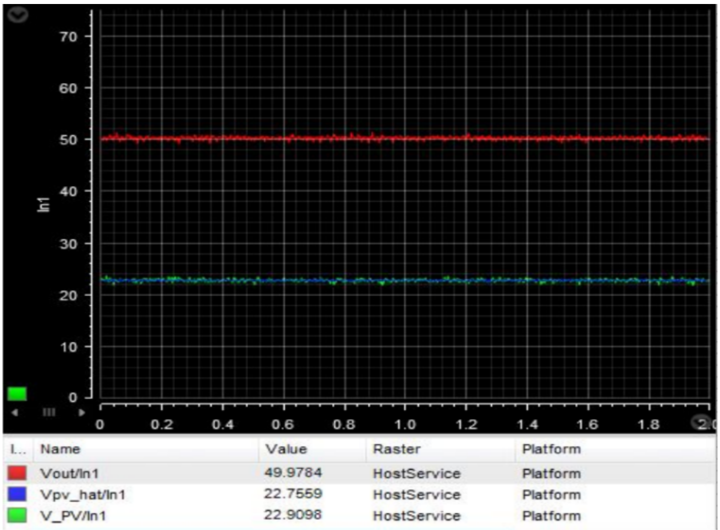

Figure 18: System voltages evolution in experimental case 1

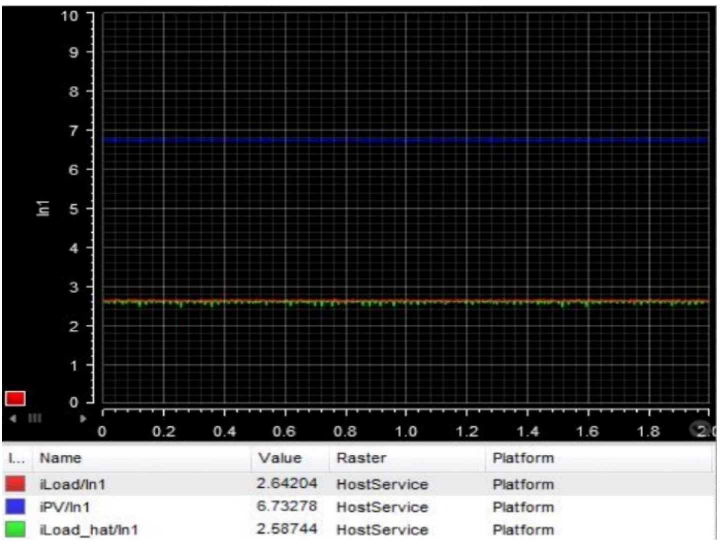

Figure 19: System currents evolution in experimental case 1

5.2.2. Experimental Case 2

For this case, the PV system is subjected to dynamic load changes under the same climatic conditions as the previous scenario.

In Case 2, the controller maintains optimal power extraction (Fig. 20) by dynamically adjusting the duty cycle in response to load changes. As shown in Fig. 23 and Fig. 24, the adaptive scheme successfully ensures exact tracking of the estimated load current and robust voltage estimation throughout these disturbances.

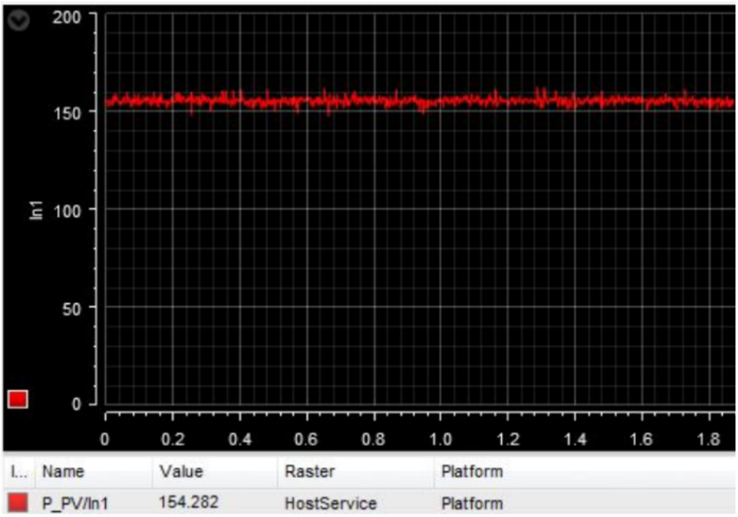

Figure 20: Photovoltaic power evolution in experimental case 2

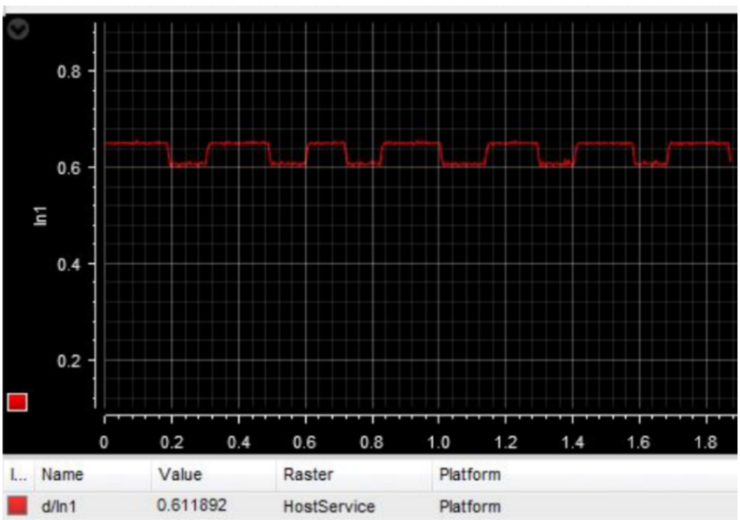

Figure 21: Duty-cycle evolution in experimental case 2

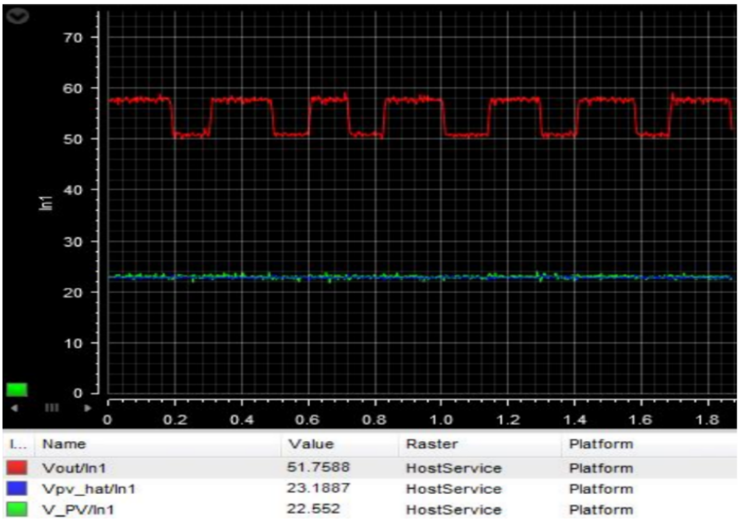

Figure 22: System voltages evolution in experimental case 2

Figure 23: System currents evolution in experimental case 2

5.2.3. Experimental Case 3

This case evaluates the system's performance under a partial shading condition, whose P–V characteristic is the blue curve shown in Fig. 15.

The ASC controller effectively handles partial shading conditions under reduced irradiance by maximizing power extraction through adaptive duty cycle control, as shown in Fig. 24 and Fig. 25. Furthermore, the accurate state estimation achieved under these challenging conditions, demonstrated in Fig. 26 and Fig. 27, validates the observer's robustness to system disturbances and uncertainties.

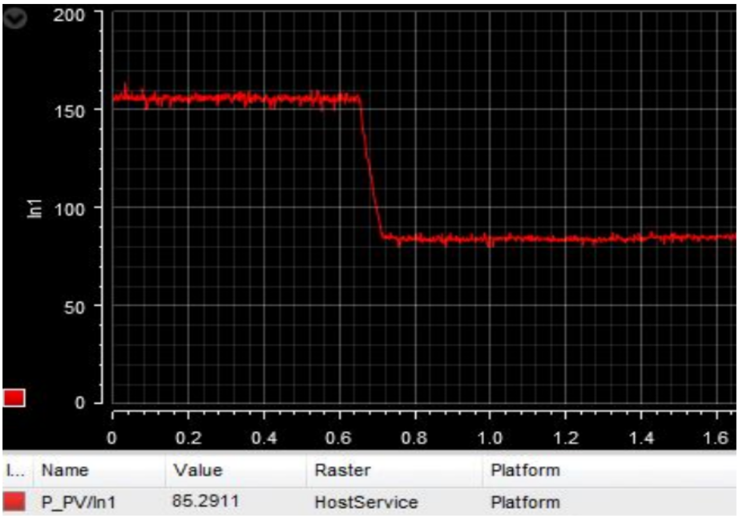

Figure 24: Photovoltaic power evolution in experimental case 3

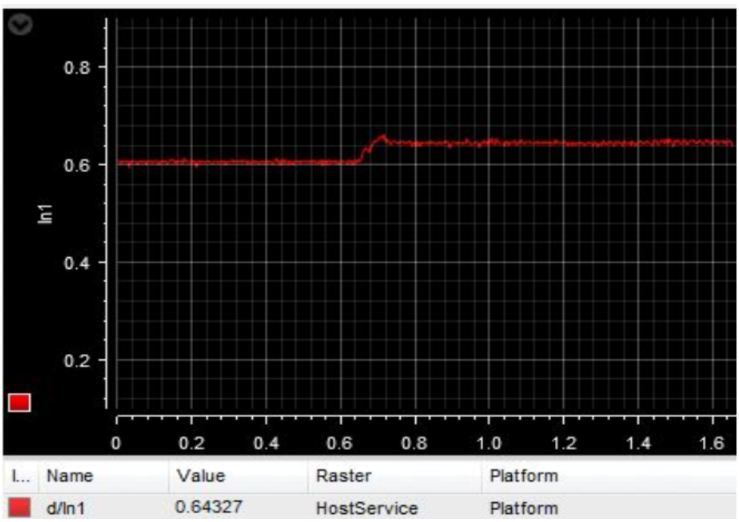

Figure 25: Duty-cycle evolution in experimental case 3

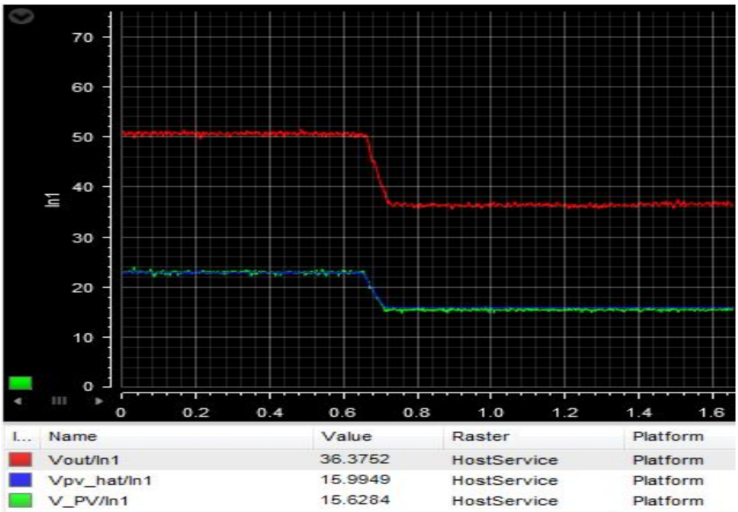

Figure 26: System voltages evolution in experimental case 3

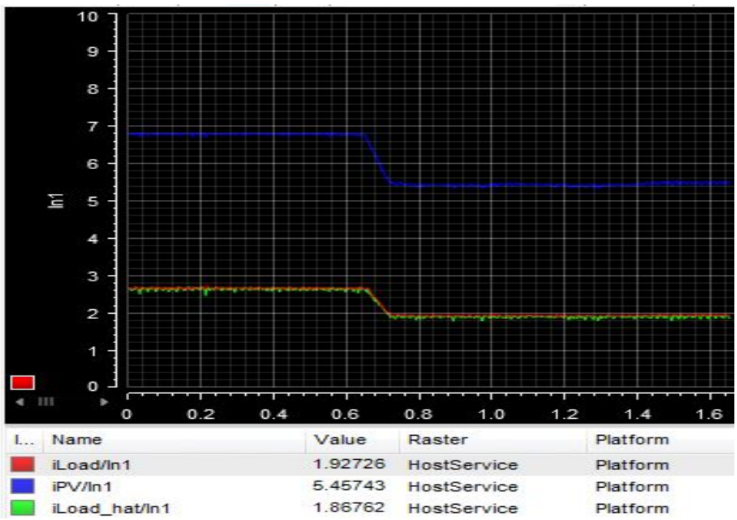

Figure 27: System currents evolution in experimental case 3

6. Conclusions

An adaptive synergetic MPPT controller, based on the robustness of both synergetic control and adaptive estimation, has been proposed in this paper. The control law has been introduced by using methods of synergetic control theory, and adaptive observer laws were used to reduce hardware complexity and avoid control-law singularities. This combination provides accurate real-time estimates of unmeasured variable states, enabling reliable control under parameter uncertainties and environmental disturbances. Simulation studies under various operating conditions demonstrated that the ASC-MPPT achieves faster convergence, reduced steady-state oscillations, and improved disturbance rejection compared to conventional synergetic approaches. Experimental validation in a practical test confirmed these results, showing consistent maximum power extraction and robust tracking performance, including in partial shading scenarios. The proposed ASC-MPPT strategy offers a low-cost, computationally efficient, and robust solution suitable for real-time implementation in modern photovoltaic conversion systems.

References

[1] S. Chen, J. Zhang, Z. Wei, H. Cheng, and S. Lv: Towards renewable-dominated energy systems: role of green hydrogen. *Journal of Modern Power Systems and Clean Energy*, **12**(6), (2024), 1697–1709. DOI: 10.35833/mpce.2023.000887

[2] T.Z. Ang, M. Salem, M. Kamarol, H.S. Das, M.A. Nazari, and N. Prabaharan: A comprehensive study of renewable energy sources: Classifications, challenges and suggestions. *Energy Strategy Reviews*, **43**(2022), 100939. DOI: 10.1016/j.esr.2022.100939

[3] Q. Sui, J. Zhang, J. Li, Z. Li, C. Su, and C. Liu: Optimal scheduling for renewable power grid and vessel-based hydrogen chain integrated systems considering flexible energy transfer. *Applied Energy*, **367**, (2024), 123401. DOI: 10.1016/j.apenergy.2024.123401

[4] Q. Sui, F. Wei, C. Wu, X. Lin, and Z. Li: Day-ahead energy management for pelagic island microgrid groups considering non-integer-hour energy transmission. *IEEE Transactions on Smart Grid*, **11**(6), (2020), 5249–5259. DOI: 10.1109/TSG.2020.2994236

[5] L. Zhang, et al.: An online maximum power point capturing technique for high-efficiency power generation of solar photovoltaic systems. *Journal of Modern Power Systems and Clean Energy*, **7**(2), (2018), 357–368. DOI: 10.1007/s40565-018-0440-2

[6] M.A. Green, et al.: Solar cell efficiency tables (Version 64). *Progress in Photovoltaics Research and Applications*, **32**(7), (2024), 425–441. DOI: 10.1002/pip.3831

[7] M.E. Girgis and N.A. Elkhateeb: Enhancing photovoltaic MPPT with P&O algorithm performance based on adaptive PID control using exponential forgetting recursive least squares method. *Renewable Energy*, **237**, (2024), 121801. DOI: 10.1016/j.renene.2024.121801

[8] S.K. Kollimalla and M.K. Mishra: Variable perturbation size adaptive P&O MPPT algorithm for sudden changes in irradiance. *IEEE Transactions on Sustainable Energy*, **5**(3), (2014), 718–728. DOI: 10.1109/tste.2014.2300162

[9] N. Kumar, I. Hussain, B. Singh, and B.K. Panigrahi: Self-Adaptive Incremental Conductance Algorithm for swift and Ripple-Free maximum power harvesting from PV array. *IEEE Transactions on Industrial Informatics*, **14**(5), (2017), 2031–2041. DOI: 10.1109/tii.2017.2765083

[10] N. Zhani and H. Mahmoudi: Comparison of the performance of MPPT control techniques (Fuzzy Logic, Incremental Conductance and Perturb & Observe) under MATLAB/Simulink. *IFAC-PapersOnLine*, 58(13), (2024), 617–623. DOI: 10.1016/j.ifacol.2024.07.551

[11] A. Talha, H. Boumaaraf, and O. Bouhali: Evaluation of maximum power point tracking methods for photovoltaic systems. *Archives of Control Sciences*, **21**(2), (2011), 151–165. DOI: 10.2478/v10170-010-0037-0

[12] A.K. Podder, N.K. Roy, and H.R. Pota: MPPT methods for solar PV systems: a critical review based on tracking characteristics. *IEEE Access*, **7**, (2019), 132517–132539. DOI: 10.1109/ACCESS.2019.2939872

[13] A. Guerbouz, et al.: Advanced sliding mode control for optimal grid integration of PV systems. *Energy Reports*, **14**, (2025), 4246–4274. DOI: 10.1016/j.egyr.2025.11.014

[14] B. Subudhi and P.S. Ogeti: Sliding mode approach to torque and pitch control for an wind energy system using FPGA. *Archives of Control Sciences*, **22**(3), (2012) 285–302. DOI: 10.2478/v10170-011-0025-z

[15] A. Hadjira, B. Khalissa, B. Ziyad, and Z. Nadjat: MPPT for photovoltaic system using adaptive fuzzy backstepping sliding mode control. *European Journal of Electrical Engineering*, **23**(5), (2021), 391–399. DOI: 10.18280/ejee.230505

[16] M.A. Hessad, Z. Bouchama, S. Benaggoune, and K. Behih: Cascade sliding mode maximum power point tracking controller for photovoltaic systems. *Electrical Engineering & Electromechanics*, **1**, (2023), 51–56. DOI: 10.20998/2074-272x.2023.1.07

[17] A.-B.A. Al-Hussein, F.R. Tahir, and V.-T. Pham: FPGA implementation of synergetic Controller-Based MPPT algorithm for a standalone PV system. *Computation*, **13**(3), (2025), 64. DOI: 10.3390/computation13030064

[18] N. Patil and R.M. Linus: Optimal synergetic control using chaotic dragon fly-based MPPT with cascaded ANFIS method for ultrafast electric vehicle charging by hybrid RES systems. *Electrical Engineering*, **106**(6), (2024), 7465–7489. DOI: 10.1007/s00202-024-02447-z

[19] A. Taissala, et al.: An Optimized Synergetic Nonlinear Controller (OSNC) based maximum power point tracking for a standalone photovoltaic system using a boost converter. *Energy Reports*, **8**, (2022), 107–122. DOI: 10.1016/j.egyr.2022.06.094

[20] N. Drir, L. Barazane, and M. Loudini: Optimizing the operation of a photovoltaic generator by a genetically tuned fuzzy controller. *Archives of Control Sciences*; **23**(2), (2013), 145–167. DOI: 10.2478/acsc-2013-0009

[21] Y. Belkhier, A. Oubelaid, and N.S. Bajaj: Experimental validation of synergetic MPPT controller for PV system using dSPACE DS1104. *Energy Reports*, **9**, (2023), 245–256. DOI: 10.1016/j.egyr.2023.01.123

[22] F. Messaoudi, et al.: Improved Synergetic MPPT Controller via Dual Loop Control for a Standalone PV System. *Optimal Control Applications and Methods*, 46(5), (2025), 2067–2081. DOI: 10.1002/oca.3308

[23] R. Ayat, A. Bouafia, and J. Gaubert: Experimental validation of synergetic approach based MPPT controller for an autonomous PV system. *IET Renewable Power Generation*, **15**(7), (2021), 1515–1527. DOI: 10.1049/rpg2.12130

[24] K. Bentata, A. Mohammedi, and T. Benslimane: Development of rapid and reliable cuckoo search algorithm for global maximum power point tracking of solar PV systems in partial shading condition. *Archives of Control Sciences*, **31**(3), (2021), 495–526. DOI: 10.24425/acs.2021.138690

[25] J.P. La Salle: *The stability of dynamical systems*. 1976. DOI: 10.1137/1.9781611970432

[26] A.M. Shaheen, et al.: Optimal parameters extraction of photovoltaic triple diode model using an enhanced artificial gorilla troops optimizer. *Energy*, **283,** (2023), 129034. DOI: 10.1016/j.energy.2023.129034

[27] S.R. Pendem and S. Mikkili: Modeling, simulation and performance analysis of solar PV array configurations (Series, Series–Parallel and Honey-Comb) to extract maximum power under Partial Shading Conditions. *Energy Reports*, **4**, (2018), 274–287. DOI: 10.1016/j.egyr.2018.03.003